

Multi-Stage Speech Bandwidth Extension with Flexible Sampling Rate Control

Ye-Xin Lu, Yang Ai, Zheng-Yan Sheng, Zhen-Hua Ling

National Engineering Research Center of Speech and Language Information Processing,
University of Science and Technology of China, Hefei, P. R. China

{yxl0102, zysheng}@mail.ustc.edu.cn, {yangai, zhling}@ustc.edu.cn

Abstract

The majority of existing speech bandwidth extension (BWE) methods operate under the constraint of fixed source and target sampling rates, which limits their flexibility in practical applications. In this paper, we propose a multi-stage speech BWE model named MS-BWE, which can handle a set of source and target sampling rate pairs and achieve flexible extensions of frequency bandwidth. The proposed MS-BWE model comprises a cascade of BWE blocks, with each block featuring a dual-stream architecture to realize amplitude and phase extension, progressively painting the speech frequency bands stage by stage. The teacher-forcing strategy is employed to mitigate the discrepancy between training and inference. Experimental results demonstrate that our proposed MS-BWE is comparable to state-of-the-art speech BWE methods in speech quality. Regarding generation efficiency, the one-stage generation of MS-BWE can achieve over one thousand times real-time on GPU and about sixty times on CPU.

Index Terms: speech bandwidth extension, multi-stage extension, amplitude prediction, phase prediction, teacher-forcing

1. Introduction

Speech bandwidth extension (BWE) aims to supplement the high-frequency components of narrowband speech signals, expanding the frequency bandwidth to enhance speech quality and intelligibility. Traditional speech BWE methods utilized signal processing techniques to predict high-frequency residual signals and spectral envelopes, including source-filter-based methods [1, 2], mapping-based methods [3–5], and statistic methods [6–9]. However, these conventional methods suffered from bottlenecks in terms of model capabilities, resulting in the generation of over-smoothed spectral parameters [10].

With the development of deep learning, deep neural networks (DNNs) with powerful modeling capabilities were increasingly applied in the field of speech BWE. DNN-based speech BWE methods can be broadly categorized into time-domain methods and frequency-domain methods. In the category of time-domain methods, mapping-based methods learned the direct mapping from narrowband speech waveforms to their wideband counterparts [11–14], while gradient-based methods leveraged diffusion models to recover wideband speech waveforms from the noised narrowband ones progressively [15–17]. In the frequency-domain category, vocoder-based methods adopted neural vocoders to recover the wideband speech waveforms from the extended mel-spectrograms [18]. Spectrum-based methods chose to directly predict the wideband time-frequency transformed spectra [19–21] from the narrowband ones and used inverse transformation to reconstruct the wideband speech waveforms. While current speech BWE methods have exhibited promising performance, they were constrained

by predefined source and target sampling rates. Due to the varying sampling rates of speech in different practical application scenarios, establishing a separate model for each sampling rate pair would result in a significant memory footprint requirement and a lack of flexibility in model utilization.

To this end, we propose MS-BWE, a multi-stage speech BWE model that can handle flexible source and target sampling rate pairs. The proposed MS-BWE comprises a series of BWE blocks, facilitating extensions among a set of sampling rates from low to high. For each BWE block, we follow our previous work [21] to use a dual-stream architecture to predict the wideband log-amplitude and phase spectra from the narrowband counterparts derived by short-time Fourier transform (STFT). The extended speech waveforms of each BWE block can be obtained from the extended log-amplitude and phase spectra using inverse STFT (iSTFT). Furthermore, to mitigate the discrepancy between training and inference as well as achieve flexible extension across multiple stages of sampling rates, we employ the teacher-forcing strategy [22] to randomly use either the real log-amplitude and phase spectra or the generated ones from the prior BWE block as the input of current BWE block with scheduled sampling. Experimental results demonstrate that our proposed MS-BWE is comparable to the state-of-the-art (SOTA) speech BWE methods in speech quality across flexible sampling rates with a unified model. In terms of generation efficiency, the one-stage generation of our proposed MS-BWE can generate 48 kHz waveform samples 1271.81 times faster than real-time on a single NVIDIA RTX 4090 GPU and 59.70 times faster than real-time on a single CPU.

2. Methodology

2.1. Overview

The overall structure of the proposed MS-BWE is illustrated in Fig. 1. Given a set of sampling rates $\mathcal{S} = \{S_0, S_1, \dots, S_N\}$ Hz, where $S_0 < S_1 < \dots < S_N$, the proposed MS-BWE aims to realize flexible extension between any source and target sampling rate pair (S_i, S_j) , $0 \leq i < j \leq N$. To achieve this, the proposed MS-BWE comprises N BWE blocks, with each block sequentially implementing the extension between adjacent sampling rates. Following our previously proposed AP-BWE [21], we design each BWE block to extend the speech waveforms at the spectral level through parallel amplitude and phase streams.

During the training stage, the narrowband waveform with a sampling rate of S_0 Hz is first interpolated to a narrowband waveform with the sampling rate of S_N using a sinc filter. Subsequently, the corresponding narrowband amplitude and phase spectra are extracted from the sinc-interpolated narrowband waveform through STFT and then fed to the first BWE block. For the n -th BWE block, where $1 < n \leq N$, it ran-

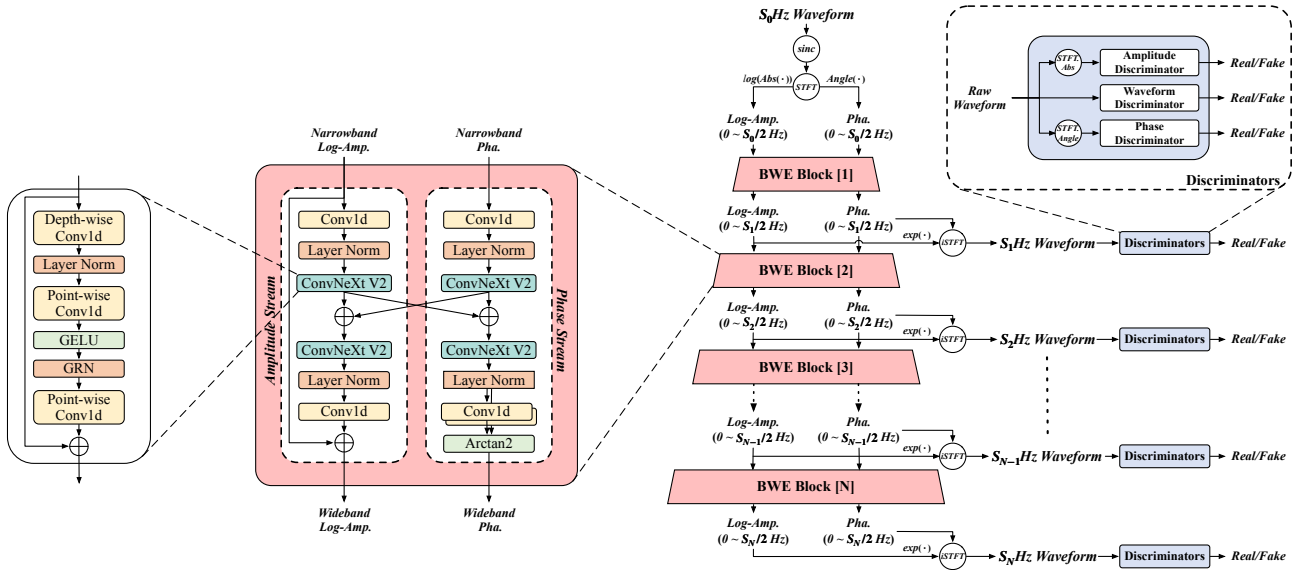


Figure 1: Overall structure of the proposed MS-BWE. The sinc denotes the sinc filter interpolation, $\text{Abs}(\cdot)$ and $\text{Angle}(\cdot)$ denote the amplitude and phase calculation functions, $\log(\cdot)$ and $\exp(\cdot)$ denote the logarithmic and exponential functions, and $(0 \sim S_n/2 \text{ Hz})$, $n \in \{0, 1, \dots, N\}$ denotes that the effective frequency bands of the amplitude and phase spectra range from 0 to $S_n/2$ Hz.

domly samples either the real log-amplitude and phase spectra extracted from the sinc-interpolated S_{n-1} Hz waveform or the generated ones from the previous BWE block as inputs. At the inference stage, for the speech BWE from a source sampling rate of S_i Hz to a target sampling rate of S_j Hz, the narrowband S_i Hz waveform first undergoes sinc interpolation and then STFT to extract the narrowband log-amplitude and phase spectra, which are then fed into the $(i+1)$ -th BWE block. After undergoing $(j-i)$ stages of generation, the j -th BWE block outputs the extended log-amplitude and phase spectra with the effective bandwidth of $S_j/2$ Hz, which are further transformed back into a S_j Hz waveform via iSTFT. The details of the model structure and training criteria are described as follows.

2.2. Model structure

As depicted in Fig 1, the proposed MS-BWE comprises a cascade of BWE blocks, each taking a pair of narrowband log-amplitude spectrum and phase spectrum as inputs and generating the corresponding extended spectra through parallel amplitude and phase streams. Both the amplitude stream and the phase stream utilize the ConvNeXt V2 [23] as their foundational backbone. Similar to the ConvNeXt [24] used in AP-BWE [21], the ConvNeXt V2 features a depth-wise convolutional layer and a pair of point-wise convolutional layers, interleaved with layer normalization [25] and Gaussian error linear unit (GELU) activation [26]. Differently, ConvNeXt V2 added a new global response normalization (GRN) layer after the GELU activation to enhance inter-channel feature competition.

On the basis of ConvNeXt V2, the amplitude stream and phase stream share a similar architecture. Each stream consists of two ConvNeXt V2 blocks and employs two convolutional layers with layer normalization on both sides for feature-dimensionality expansion and restoration, respectively. For the amplitude stream, the output convolutional layer predicts the residual log-amplitude spectrum, which is subsequently added to the input narrowband one to obtain the extended log-amplitude spectrum. Nevertheless, due to the phase-wrapping

issue, the phase stream utilizes the parallel wrapped phase estimation architecture [27] to predict the extended phase spectrum directly, which comprises two parallel convolutional layers to output the pseudo-real part and imaginary part components and further calculate the wrapped phase spectrum with the activation of the two-argument arc-tangent (Arctan2) function.

2.3. Training criteria

2.3.1. Loss functions

To avoid the generation of over-smoothed spectra, we employ the training approach of the generative-adversarial network (GAN) to define N sets of discriminators on the extended speech waveforms of the N BWE blocks. Within each set of the discriminators, we first define the waveform discriminator at the waveform level, which derives from the sub-discriminator of the multi-scale discriminator [28,29]. Furthermore, we respectively define the amplitude discriminator and phase discriminator to enhance the realism of extended amplitude and phase spectra, which are borrowed from the sub-discriminators of the multi-resolution amplitude and phase discriminators [21].

We use the hinge GAN loss [30] to jointly train the MS-BWE model and the discriminators. For the generator loss, besides the GAN losses, we follow AP-BWE [21] to define spectral losses on the outputs of each BWE block, including log-amplitude mean square error (MSE) loss, phase anti-wrapping losses [27], and short-time complex spectral MSE loss.

2.3.2. Teacher-forcing strategy

Since the speech BWE process is carried out stage by stage, it can lead to two types of mismatch between training and inference: 1) In the training stage, each BWE block only samples the real amplitude and phase as inputs, i.e., the N BWE blocks are trained separately. For the inference from S_i Hz to S_j Hz, if $j-i > 1$, the $i+2, i+3, \dots, j$ -th BWE block need to receive the outputs of the previous block as inputs, which mismatches with the real inputs in training. 2) In the training stage, the n -th BWE block only samples the generated amplitude and phase

Table 1: Experimental results for BWE methods evaluated on the VCTK-0.92 dataset with the target sampling rate of 48 kHz, where in RTF ($a\times$) represents a times real-time and n represents the n -stage generation. The **bold** and underlined numbers indicate the optimal and sub-optimal results, respectively.

Method	8 kHz \rightarrow 48 kHz		12 kHz \rightarrow 48 kHz		16 kHz \rightarrow 48 kHz		24 kHz \rightarrow 48 kHz		RTF (CPU)	RTF (GPU)
	LSD	ViSQOL	LSD	ViSQOL	LSD	ViSQOL	LSD	ViSQOL		
sinc	2.94	2.07	2.75	2.09	2.57	2.26	2.17	2.99	-	-
NU-Wave2 [16]	1.09	2.48	0.94	2.75	0.86	3.00	0.72	3.74	92.5836 (0.01 \times)	0.5195 (1.92 \times)
UDM+ [17]	1.03	2.81	0.88	3.08	0.79	3.35	0.64	4.02	74.0332 (0.01 \times)	0.8335 (1.20 \times)
mdctGAN [20]	0.93	2.95	0.90	2.96	0.82	3.15	0.72	3.58	0.2461 (4.06 \times)	0.0129 (77.80 \times)
AP-BWE [21]	0.85	3.32	0.79	3.46	0.72	<u>3.63</u>	0.62	4.17	0.0551 (18.14 \times)	0.0034 (292.28 \times)
MS-BWE	0.85	<u>3.31</u>	0.79	<u>3.44</u>	<u>0.73</u>	3.65	<u>0.63</u>	<u>4.14</u>	0.0167 * n (59.70 / $n \times$)	0.0008 * n (1271.81 / $n \times$)

from the $(n - 1)$ -th block as inputs, where $1 < n \leq N$. For the inference from S_i Hz to S_j Hz, if $j > i > 1$, the $(i + 1)$ -th BWE block needs to receive the real amplitude and phase as inputs, which mismatches with the generated inputs in training.

In order to address these two types of mismatch issues, we propose to employ the teacher-forcing strategy with schedule sampling [22]. During the training stage, except for the first BWE block, the remaining blocks randomly sample their inputs from either the real amplitude and phase or the extended ones from the previous block with a ratio. This teacher-forcing ratio is scheduled to decrease progressively every mini-batch, transitioning the model from relying more on real samples to using more generated samples. This strategic shift aids the model in better adapting to its own generated outputs, consequently mitigating the discrepancy between training and inference.

3. Experiments

3.1. Datasets and experimental setup

We used the publicly available VCTK-0.92 dataset [31] for our experiments, which contains about 44 hours of speech recording at a sampling rate of 48 kHz from 110 speakers. Following the same configuration of previous works [16, 17], we split the data into training and test sets. The experiments were performed with commonly used sampling rates, where $\mathbb{S} = \{8000, 12000, 16000, 24000, 48000\}$ and consequently $N = 4$. To obtain narrowband speech signals, we downsampled the 48 kHz speech waveforms with the sinc filter to decimate the high-frequency components without any alias.

For training the MS-BWE model, all the speech recordings were sliced into 8000-sample-point clips and subsequently processed by STFT to extract amplitude and phase spectrum with the FFT point number, Hanning window size, and hop size of 1024, 320, and 80, respectively. The teacher-forcing ratio was set initially to 0.75 and scheduled to decay with a factor of 0.999995 every mini-batch, where the batch size was set to 16. The MS-BWE model was trained until 500k steps using the Adam optimizer [32] with $\beta_1 = 0.8$, $\beta_2 = 0.99$, and weight decay $\lambda = 0.01$. The learning rate was set initially to 2×10^{-4} and scheduled to decay with a factor of 0.999 every epoch.¹

3.2. Baseline methods

We first used the sinc filter interpolation as the lower-bound baseline, and compared our proposed MS-BWE with two diffusion-based methods (NU-Wave 2 [16] and UDM+ [17]),

¹Audio samples of the proposed MS-BWE can be accessed at <https://yxlx-0102.github.io/MS-BWE-demo>.

a modified discrete cosine transform (MDCT) spectrum-based method (mdctGAN [20]), and an amplitude-phase spectrum-based method (AP-BWE [21]). For the common experiments targeting 48 kHz, we first used the reproduced NU-Wave 2 checkpoint and the official UDM+ checkpoint in UDM+'s official implementation². We further adopted the official checkpoints of mdctGAN and the unified AP-BWE in their open-source implementations^{3,4}, and re-trained them for experiments with other pairs of source and target sampling rates.

3.3. Evaluation metrics

For extended speech quality evaluation, we first utilized the commonly used log-spectral distance (LSD) as the objective evaluation metric. Additionally, we employed the virtual speech quality objective listener (ViSQOL) [33] to evaluate the overall speech quality, which ranges from 1 to 4.75 at 16 kHz and from 1 to 5 at 48 kHz. For speech signals extended to 12 kHz or 24 kHz, we respectively resampled them to 16 kHz and 48 kHz to evaluate the ViSQOL score. For LSD, lower values indicate better performance, while for ViSQOL, the higher, the better. To assess generation efficiency, we used the real-time factor (RTF), which is defined as the ratio between the total inference time on the test set and the total duration of the test set. In our implementation, we calculated the RTFs on a single RTX 4090 GPU and a single Intel(R) Xeon(R) Silver 4310 CPU (2.10 GHz).

4. Results and Analysis

4.1. Comparison with baseline methods

4.1.1. Many-to-one speech BWE

The current mainstream methods [16, 17, 20, 21] all performed speech BWE in a many-to-one manner with multiple source sampling rates and a fixed target sampling rate. Therefore, we first compared our proposed MS-BWE with these SOTA baseline methods in this configuration. For source sampling rates of 8 kHz, 12 kHz, 16 kHz, and 24 kHz, our proposed MS-BWE respectively utilized 4, 3, 2, and 1 BWE block(s) for generations, while NU-Wave 2, UDM+, and AP-BWE utilized unified models and mdctGAN used four separate models.

As shown in Table 1, our proposed MS-BWE achieved comparable performance with AP-BWE and far surpassed other baseline methods in terms of extended speech quality. Compared to the sub-optimal mdctGAN, the MS-BWE exhibited significant improvements of 8.6%, 12.2%, 10.9%, and 12.5% in

²<https://github.com/yoyololicon/diffwave-sr>.

³<https://github.com/neoncloud/mdctGAN>.

⁴<https://github.com/yxlx-0102/AP-BWE>.

Table 2: Experimental results for BWE methods evaluated on the VCTK-0.92 dataset with flexible source and target sampling rates, where $aM * b$ indicates b models with aM parameters each are required for all the speech BWE implementations.

Method	8 kHz \rightarrow 12 kHz		8 kHz \rightarrow 16 kHz		8 kHz \rightarrow 24 kHz		12 kHz \rightarrow 16 kHz		12 kHz \rightarrow 24 kHz		16 kHz \rightarrow 24 kHz		# Param.
	LSD	ViSQOL	LSD	ViSQOL	LSD	ViSQOL	LSD	ViSQOL	LSD	ViSQOL	LSD	ViSQOL	
mdctGAN	0.64	4.72	0.78	4.57	0.89	3.79	0.55	4.81	0.75	3.86	0.66	4.03	103M * 6
AP-BWE	0.62	4.81	<u>0.73</u>	4.69	<u>0.83</u>	3.87	0.55	4.89	0.72	3.96	<u>0.61</u>	4.11	30M * 3
MS-BWE	0.62	<u>4.74</u>	0.72	<u>4.59</u>	0.82	<u>3.81</u>	<u>0.56</u>	<u>4.82</u>	<u>0.74</u>	<u>3.90</u>	0.59	<u>4.08</u>	43M * 1

LSD as well as 12.2%, 16.2%, 15.8%, and 15.6% in ViSQOL for source sampling rates of 8 kHz, 12 kHz, and 16 kHz, and 24 kHz, respectively. Compared to AP-BWE, the performance of MS-BWE was slightly inferior, which may be attributed to the simultaneous optimizations of multiple training objectives in our model. In terms of generation efficiency, although AP-BWE has achieved at least four times faster than other baselines, it still employed a unified model for all source sampling rates, resulting in the wastage of model parameters. For our proposed MS-BWE, the efficiency of one-stage generation (e.g., 24 kHz \rightarrow 48 kHz) can reach an approximately fourfold acceleration than that of AP-BWE on both GPU and CPU. This notable enhancement was attributed to the fact that, for the one-stage generation, MS-BWE saved nearly $3/4$ of the parameters compared to AP-BWE, achieving a more efficient parameter utilization. Similarly, the n -stage generation of our proposed MS-BWE can generate 48 kHz waveform samples about $1271.81/n$ times faster than real-time on a single GPU and about $59.70/n$ times faster than real-time on a single CPU.

4.1.2. Many-to-many speech BWE

We further compared our proposed MS-BWE with two optimal baseline methods (i.e., mdctGAN and AP-BWE) in a many-to-many manner of speech BWE to evaluate our method’s flexibility. As shown in Table 2, our proposed MS-BWE apparently outperformed mdctGAN, and performed comparably to AP-BWE in LSD but lagged behind in ViSQOL, which was consistent with the results in Table 1. It is noteworthy that, for the sampling rate set $\mathbb{S} = \{S_0, S_1, \dots, S_N\}$, the approaches which can only handle one pair of source and target sampling rates at a time (e.g., mdctGAN), required $\frac{N^2+N}{2}$ individual models to achieve all the extensions between these sampling rates. Even for methods that can simultaneously handle multiple source sampling rates (e.g., AP-BWE), at least N independent models were still required. Nevertheless, our proposed MS-BWE demonstrated the ability to realize flexible extensions across the sampling rate set using a unified model, while maintaining comparable performance to these individual baseline models. Therefore, as shown in Table 2, the total parameter requirement for all speech BWE implementations of our model was significantly lower than the other two baseline models, allowing it to be flexibly applied to resource-constrained scenarios.

4.2. Analysis on training strategies

To verify the effectiveness of the teacher-forcing strategy on the overall model performance, we conducted analysis experiments by using different training strategies, and the experimental results are presented in Table 3. Initially, we trained the MS-BWE model without sampling from its own generated intermediate results (denoted as “Never Sampling”). In this scenario, each BWE block was trained separately using real narrowband and wideband spectra pairs. The results indicated that this train-

Table 3: Experimental results for the analysis of different training strategies with the target sampling rate of 48 kHz.

Training Strategy	8kHz \rightarrow 48kHz		16kHz \rightarrow 48kHz		24kHz \rightarrow 48kHz	
	LSD	ViSQOL	LSD	ViSQOL	LSD	ViSQOL
Never Sampling	0.97	2.95	0.75	3.50	0.61	4.23
Always Sampling	0.87	3.20	0.82	3.47	0.77	3.77
Scheduled Sampling	0.85	3.31	0.73	3.65	0.63	4.14

ing strategy yielded optimal performance for one-stage generation (e.g., 24 kHz \rightarrow 48 kHz), while the prediction errors accumulated as the number of stages increased, corresponding to the first type of mismatch discussed in Section 2.3.2. Subsequently, we trained the model to always sample from its own generated spectra (denoted as “Always Sampling”). In contrast to the “Never Sampling” scenario, the experimental results demonstrated that the model performed well for the whole N -stage generation task (i.e., 8 kHz \rightarrow 48 kHz), while the performance gradually collapsed as the number of the generation stages decreased, aligning with the second type of mismatch mentioned in Section 2.3.2. Ultimately, with the implementation of the teacher-forcing strategy with scheduled sampling (denoted as “Scheduled Sampling”), the model achieved a trade-off in multi-stage generation tasks by sampling from either the generated or real amplitude and phase spectra with a scheduled ratio. While it may not achieve optimal performance in each one-stage task, this approach resulted in flexible and relatively high-quality extension across the sampling rate set.

5. Conclusions

In this paper, we proposed MS-BWE, a multi-stage speech BWE model that achieves flexible extensions of a sampling rate set from low to high. The proposed MS-BWE model was GAN-based, the generator of which consisted of multiple BWE blocks, each comprising parallel amplitude and phase streams to explicitly predict the high-frequency amplitude and phase components from the narrowband spectra. Discriminators were employed on the outputs of each BWE block to further enhance the realism of each extended speech waveform at both the waveform level and the spectral level. To mitigate the discrepancy between training and inference, we employed the teacher-forcing strategy to randomly introduce the real amplitude and phase to the intermediate BWE blocks. Experimental results demonstrated that our proposed MS-BWE performed comparably to the SOTA baseline methods in flexible speech BWE tasks with a unified model while ensuring remarkable efficiency. In summary, through the stage-wise speech BWE process, our method made full use of the model parameters and demonstrated the potential for practical applications in resource-constrained scenarios.

6. References

- [1] J. Makhoul and M. Berouti, "High-frequency regeneration in speech coding systems," in *Proc. ICASSP*, vol. 4, 1979, pp. 428–431.
- [2] S. Chennoukh, A. Gerrits, G. Miet, and R. Sluijter, "Speech enhancement via frequency bandwidth extension using line spectral frequencies," in *Proc. ICASSP*, vol. 1, 2001, pp. 665–668.
- [3] H. Carl, "Bandwidth enhancement of narrowband speech signals," in *Proc. EUSIPCO*, vol. 2, 1994, pp. 1178–1181.
- [4] T. Unno and A. McCree, "A robust narrowband to wideband extension system featuring enhanced codebook mapping," in *Proc. ICASSP*, vol. 1, 2005, pp. 1–805.
- [5] J. Sadasivan, S. Mukherjee, and C. S. Seelamantula, "Joint dictionary training for bandwidth extension of speech signals," in *Proc. ICASSP*, 2016, pp. 5925–5929.
- [6] H. Pulakka, U. Remes, K. Palomäki, M. Kurimo, and P. Alku, "Speech bandwidth extension using Gaussian mixture model-based estimation of the highband mel spectrum," in *Proc. ICASSP*, 2011, pp. 5100–5103.
- [7] G. Chen and V. Parsa, "HMM-based frequency bandwidth extension for speech enhancement using line spectral frequencies," in *Proc. ICASSP*, vol. 1, 2004, pp. 1–709.
- [8] Y. Ohtani, M. Tamura, M. Morita, and M. Akamine, "GMM-based bandwidth extension using sub-band basis spectrum model," in *Proc. Interspeech*, 2014, pp. 2489–2493.
- [9] G.-B. Song and P. Martynovich, "A study of HMM-based bandwidth extension of speech signals," *Signal Processing*, vol. 89, no. 10, pp. 2036–2044, 2009.
- [10] Z.-H. Ling, S.-Y. Kang, H. Zen, A. Senior, M. Schuster, X.-J. Qian, H. M. Meng, and L. Deng, "Deep learning for acoustic modeling in parametric speech generation: A systematic review of existing techniques and future trends," *IEEE Signal Processing Magazine*, vol. 32, no. 3, pp. 35–52, 2015.
- [11] V. Kuleshov, S. Z. Enam, and S. Ermon, "Audio super-resolution using neural nets," in *Proc. ICLR (Workshop Track)*, 2017.
- [12] Z.-H. Ling, Y. Ai, Y. Gu, and L.-R. Dai, "Waveform modeling and generation using hierarchical recurrent neural networks for speech bandwidth extension," *IEEE/ACM Transactions on Audio, Speech, and Language Processing*, vol. 26, no. 5, pp. 883–894, 2018.
- [13] S. Birnbaum, V. Kuleshov, Z. Enam, P. W. W. Koh, and S. Ermon, "Temporal FiLM: Capturing long-range sequence dependencies with feature-wise modulations," *Proc. NeurIPS*, vol. 32, 2019.
- [14] N. C. Rakotonirina, "Self-attention for audio super-resolution," in *Proc. MLSP*, 2021, pp. 1–6.
- [15] J. Lee and S. Han, "NU-Wave: A diffusion probabilistic model for neural audio upsampling," *Proc. Interspeech*, pp. 1634–1638, 2021.
- [16] S. Han and J. Lee, "NU-Wave 2: A general neural audio upsampling model for various sampling rates," in *Proc. Interspeech*, 2022, pp. 4401–4405.
- [17] C.-Y. Yu, S.-L. Yeh, G. Fazekas, and H. Tang, "Conditioning and sampling in variational diffusion models for speech super-resolution," in *Proc. ICASSP*, 2023, pp. 1–5.
- [18] H. Liu, W. Choi, X. Liu, Q. Kong, Q. Tian, and D. Wang, "Neural vocoder is all you need for speech super-resolution," in *Proc. Interspeech*, 2022, pp. 4227–4231.
- [19] M. Mandel, O. Tal, and Y. Adi, "AERO: Audio super resolution in the spectral domain," in *Proc. ICASSP*, 2023, pp. 1–5.
- [20] C. Shuai, C. Shi, L. Gan, and H. Liu, "mdctGAN: Taming transformer-based GAN for speech super-resolution with modified DCT spectra," in *Proc. Interspeech*, 2023, pp. 5112–5116.
- [21] Y.-X. Lu, Y. Ai, H.-P. Du, and Z.-H. Ling, "Towards high-quality and efficient speech bandwidth extension with parallel amplitude and phase prediction," *arXiv preprint arXiv:2401.06387*, 2024.
- [22] S. Bengio, O. Vinyals, N. Jaitly, and N. Shazeer, "Scheduled sampling for sequence prediction with recurrent neural networks," in *Proc. NeurIPS*, vol. 28, 2015, pp. 1171–1179.
- [23] S. Woo, S. Debnath, R. Hu, X. Chen, Z. Liu, I. S. Kweon, and S. Xie, "ConvNeXt V2: Co-designing and scaling convnets with masked autoencoders," in *Proc. CVPR*, 2023, pp. 16 133–16 142.
- [24] Z. Liu, H. Mao, C.-Y. Wu, C. Feichtenhofer, T. Darrell, and S. Xie, "A convnet for the 2020s," in *Proc. CVPR*, 2022, pp. 11 976–11 986.
- [25] J. L. Ba, J. R. Kiros, and G. E. Hinton, "Layer normalization," *stat*, vol. 1050, p. 21, 2016.
- [26] D. Hendrycks and K. Gimpel, "Gaussian error linear units (GELUs)," in *Proc. ICML*, vol. 70, 2017, pp. 3441–3450.
- [27] Y. Ai and Z.-H. Ling, "Neural speech phase prediction based on parallel estimation architecture and anti-wrapping losses," in *Proc. ICASSP*, 2023, pp. 1–5.
- [28] K. Kumar, R. Kumar, T. De Boissiere, L. Gestin, W. Z. Teoh, J. Sotelo, A. De Brebisson, Y. Bengio, and A. C. Courville, "MelGAN: Generative adversarial networks for conditional waveform synthesis," in *Proc. NeurIPS*, vol. 32, 2019.
- [29] J. Kong, J. Kim, and J. Bae, "HiFi-GAN: Generative adversarial networks for efficient and high fidelity speech synthesis," *Proc. NeurIPS*, vol. 33, pp. 17 022–17 033, 2020.
- [30] N. Zeghidour, A. Luebs, A. Omran, J. Skoglund, and M. Tagliasacchi, "Soundstream: An end-to-end neural audio codec," *IEEE/ACM Transactions on Audio, Speech, and Language Processing*, vol. 30, pp. 495–507, 2021.
- [31] J. Yamagishi, C. Veaux, K. MacDonald *et al.*, "CSTR VCTK corpus: English multi-speaker corpus for CSTR voice cloning toolkit (version 0.92)," *University of Edinburgh. The Centre for Speech Technology Research (CSTR)*, 2019.
- [32] I. Loshchilov and F. Hutter, "Decoupled weight decay regularization," *arXiv preprint arXiv:1711.05101*, 2017.
- [33] M. Chinen, F. S. Lim, J. Skoglund, N. Gureev, F. O’Gorman, and A. Hines, "ViSQOL v3: An open source production ready objective speech and audio metric," in *Proc. QoMEX*, 2020, pp. 1–6.